

Numerical simulation of the α -effect and turbulent magnetic diffusion with molecular diffusivity

By I. T. DRUMMOND AND R. R. HORGAN

Department of Applied Mathematics and Theoretical Physics, University of Cambridge,
Silver Street, Cambridge CB3 9EW, U.K.

(Received 16 May 1985)

We extend the numerical methods of a previous paper to the study of the α -effect in a turbulent plasma. In the frozen-turbulence case the α -effect vanishes for zero molecular diffusivity. The value of α is, however, found to depend very sensitively on the molecular diffusivity. The same is true for the turbulent magnetic diffusivity β . The theoretical predictions of the first-order smoothing and the Markovian approximations are well satisfied in the appropriate limits, for both α and β .

1. Introduction

The problem of calculating the α -effect (Krause & Rädler 1980; Moffatt 1978) and the magnetic diffusivity from the statistical properties of a turbulent plasma, is largely unsolved in the important limit of large magnetic Reynolds number. In this paper we report on a numerical simulation of the process along the lines of a previous investigation by Kraichnan (1976). Our results for the α -effect confirm his where they overlap. However, we were able to extend significantly the time interval over which the simulation could be carried out. We were also able to include the effect of molecular diffusion (finite conductivity) in our calculation. The simulation, which was performed on the ICL-DAP at Queen Mary College (London), follows closely the method used in a previous paper (Drummond, Duane & Horgan 1984) which investigated turbulent diffusion of a scalar field.

In §2 we describe the velocity ensembles we used. In §3 we discuss the extension of the integration technique for stochastic differential equations required for calculating the α -parameter and the magnetic diffusivity, and in §4 we briefly review the numerical integration procedure.

The results for the important case of frozen turbulence with and without molecular diffusivity are presented in §5. Non-frozen turbulence with and without molecular diffusivity is analysed in §6. A discussion of these results is presented in §7.

2. Velocity ensemble

The velocity field is constructed in the same way as in our previous paper (Drummond *et al.* 1984). A typical velocity field has the form

$$\mathbf{u}(\mathbf{x}, t) = A \sum_{n=1}^N \{(\xi_n \cos \psi_n - \chi_n \wedge \hat{\mathbf{k}}_n \sin \psi_n) \wedge \mathbf{k}_n \cos(\mathbf{k}_n \cdot \mathbf{x} + \omega_n t) + (\chi_n \cos \psi_n + \xi_n \wedge \hat{\mathbf{k}}_n \sin \psi_n) \wedge \mathbf{k}_n \sin(\mathbf{k}_n \cdot \mathbf{x} + \omega_n t)\}. \quad (2.1)$$

Here $\{\xi_n\}$ and $\{\chi_n\}$ are independent random variables distributed uniformly over the unit sphere, $\{\omega_n\}$ are independent Gaussian random variables with variance ω_0^2 . We

give the $\{\psi_n\}$ a common value ψ , which in this paper is set to $\frac{1}{4}\pi$, yielding maximum helicity. This form guarantees that the flow is incompressible and the distribution of parameters ensures that the turbulence is homogeneous and isotropic.

For the $\{\mathbf{k}_n\}$ we consider two distributions. The first is the δ -shell model, in which each \mathbf{k}_n is distributed uniformly over a sphere of radius k_0 , and the second, the Gaussian model, in which each component of \mathbf{k}_n has a Gaussian distribution with variance k_0^2 . In each case we choose A so that the mean-square velocity is u_0^2 .

For the δ -shell we have

$$A = \left(\frac{3}{2N}\right)^{\frac{1}{2}} \frac{u_0}{k_0} \quad (2.2)$$

and
$$\langle \mathbf{u}^2 \rangle = u_0^2, \quad \langle (\nabla \wedge \mathbf{u})^2 \rangle = u_0^2 k_0^2, \quad \langle \mathbf{u} \cdot \nabla \wedge \mathbf{u} \rangle = u_0^2 k_0 \sin \psi. \quad (2.3)$$

For the Gaussian we have

$$A = \left(\frac{1}{2N}\right)^{\frac{1}{2}} \frac{u_0}{k_0}, \quad (2.4)$$

and
$$\langle \mathbf{u}^2 \rangle = u_0^2, \quad \langle (\nabla \wedge \mathbf{u})^2 \rangle = 5k_0^2 u_0^2, \quad \langle \mathbf{u} \cdot \nabla \wedge \mathbf{u} \rangle = \frac{8}{3} \left(\frac{2}{\pi}\right)^{\frac{1}{2}} u_0^2 k_0 \sin \psi. \quad (2.5)$$

The velocity correlation functions are, for the δ -shell,

$$\langle \mathbf{u}(\mathbf{x}, t) \cdot \mathbf{u}(\mathbf{x}', t') \rangle = u_0^2 \left(\frac{\sin k_0 r}{k_0 r}\right) e^{-\frac{1}{2}u_0^2(t-t')^2}, \quad (2.6)$$

and for the Gaussian

$$\langle \mathbf{u}(\mathbf{x}, t) \cdot \mathbf{u}(\mathbf{x}', t') \rangle = \frac{1}{3}u_0^2(3 - k_0^2 r^2) e^{-\frac{1}{2}k_0^2 r^2} e^{-\frac{1}{2}u_0^2(t-t')^2}, \quad (2.7)$$

where $r = |\mathbf{x} - \mathbf{x}'|$.

Note that the δ -shell correlation function has a zero at $r = \pi/k_0$ and the Gaussian at $r = \sqrt{3}/k_0$. Since we use the same k_0 ($= 6$) in both simulations we see from a consideration of the variances of the wavevectors, or from the positions of these zeros that the spatial scales for the two models differ by a factor of roughly $\sqrt{3} = 1.74$. The helicity-correlation zeros occur at $r = \pi/k_0$ again for the δ -shell and $r = 1.51/k_0$ for the Gaussian, in this case a factor of roughly 2. Since we have set $u_0^2 = 3$ in both models a corresponding factor of 2 is implied for their relative time scales.

These general dimensional considerations are mirrored very accurately in the results, showing that both models, as might be expected, behave in much the same way. We feel that this consistency between models which are analytically different enhances confidence in our numerical procedures.

3. Stochastic differential equations for $\alpha(t)$ and $\beta(t)$

The formulae for computing $\alpha(t)$ and $\beta(t)$ in a turbulent plasma have been given by Moffatt (1978) for the case of zero molecular diffusivity. They are equivalent to the following equations:

$$\alpha(t) = \frac{1}{3}\epsilon_{ijk} \langle u_i(\mathbf{X}(t), t) W_{jk}(t) \rangle; \quad (3.1)$$

and

$$\beta(t) = \alpha(t) \langle \gamma(t) \rangle - \frac{1}{6} \langle u_j(\mathbf{X}(t), t) Y_k(t) W_{kj}(t) \rangle + \frac{1}{6} \langle u_j(\mathbf{X}(t), t) Y_j(t) W_{kk}(t) \rangle, \quad (3.2)$$

where

$$\mathbf{Y}(t) = \mathbf{X}(t) - \mathbf{a}$$

and

$$\dot{\mathbf{X}} = \mathbf{u}(\mathbf{X}, t), \quad \mathbf{X}(0) = \mathbf{a}, \quad (3.3)$$

$$\dot{W}_{kj}(t) = u_{k,i}(\mathbf{X}(t), t) W_{ij}(t), \quad W_{ij}(0) = \delta_{ij}, \quad (3.4)$$

$$\dot{\gamma}(t) = \frac{1}{3}\epsilon_{ijk} u_i(\mathbf{X}(t), t) W_{jk}(t), \quad \gamma(0) = 0. \quad (3.5)$$

The effect of molecular diffusivity κ can be introduced by altering (3.3) to

$$\dot{\mathbf{X}} = \mathbf{u}(\mathbf{X}, t) + \mathbf{v}(t), \quad (3.6)$$

where $\mathbf{v}(t)$ is a randomly fluctuating velocity with a correlation function

$$\langle v_i(t) v_j(t') \rangle = 2\kappa \delta_{ij} \delta(t-t'). \quad (3.7)$$

The matrix W_{jk} is defined by (3.4) but its geometrical significance is revealed by noting that

$$W_{jk} = \frac{\partial}{\partial a_k} X_j(t, \mathbf{a}).$$

In the case of non-zero molecular diffusivity the fluctuating velocity function $\mathbf{v}(t)$ is taken as fixed during the differentiation. All other equations can be carried over unchanged provided the averaging procedure indicated by the angular brackets is extended to include averages over the molecular fluctuations represented by $\mathbf{v}(t)$. A similar approach has been used by Molchanov, Ruzmaikin & Sokoloff (1984). These molecular fluctuations, of course, have their effect on $W(t)$, $\alpha(t)$ and $\beta(t)$, through their implicit dependence on $\mathbf{X}(t)$.

For future reference we note that these results provide two opportunities for evaluating $\alpha(t)$, namely directly through (3.1) and indirectly as the slope of $\langle \gamma(t) \rangle$, since

$$\langle \gamma(t) \rangle = \int_0^t dt' \alpha(t'). \quad (3.8)$$

It is a further check on our simulation that these two methods yield consistent results.

4. Numerical integration procedure

The generalized Runge–Kutta method for integrating the stochastic differential equation (3.6) of the previous section was set out in our previous paper (Drummond *et al.* 1984). For completeness we briefly recapitulate the method here and describe the extension necessary to deal with (3.4) and (3.5). We subsequently discovered that these techniques have also been developed by Greenside and Helfand (Helfand 1979; Greenside & Helfand 1981).

The n th-order Runge–Kutta scheme for updating variables over a time step t to $t + \Delta t$ requires the introduction of a sequence of positions ($\mathbf{x}_0, \mathbf{x}_1, \dots, \mathbf{x}_n$) and times (t_0, t_1, \dots, t_n) where $\mathbf{x}_0 = \mathbf{X}(t)$ and $\mathbf{x}_n = \mathbf{X}(t + \Delta t)$, $t_0 = t$ and $t_n = t + \Delta t$, the remaining times being chosen so that

$$t_i = t + \gamma_i \Delta t, \quad (4.1)$$

and the points so that

$$\mathbf{x}_i = \mathbf{x}_0 + \sum_{j=1}^i (\alpha_{ij} \boldsymbol{\mu}_j + \beta_{ij} \boldsymbol{\varepsilon}_j), \quad (4.2)$$

where

$$\boldsymbol{\mu}_i = \mathbf{u}(\mathbf{x}_{i-1}, t_{i-1}) \Delta t \quad (4.3)$$

and

$$\boldsymbol{\varepsilon}_i = (2\kappa \Delta t)^{\frac{1}{2}} \boldsymbol{\eta}_i, \quad (4.4)$$

where $i = 1, 2, \dots, n$ and $\boldsymbol{\eta}_i$ are a set of independent random variables with zero mean and unit variance. The coefficients α_{ij} , β_{ij} and γ_i are chosen as explained in our previous paper (Drummond *et al.* 1984).

In order to integrate a set of quantities F_α obeying differential equations

$$\dot{F}_\alpha = V_\alpha(F, \mathbf{x}, t) \quad (4.5)$$

over the time interval t to $t + \Delta t$ we introduce a sequence $F_{\alpha, i}$ $i = 0, 1, \dots, n$, where $F_{\alpha, 0} = F_{\alpha}(t)$, $F_{\alpha, n} = F_{\alpha}(t + \Delta t)$ and

$$F_{\alpha, i} = \sum_{j=1}^i \alpha_{ij} V_{\alpha, j} \Delta t, \quad (4.6)$$

with

$$V_{\alpha, j} = V_{\alpha}(F_{j-1}, \mathbf{x}_{j-1}, t_{j-1}), \quad (4.7)$$

the coefficients α_{ij} being the same as above.

It is clear that the ten quantities W_{ij} , γ satisfy (see (3.4) and (3.5)) equations of the form of (4.5). We apply a third-order procedure ($n = 3$) to these equations which yields an update which is correct to $O(\Delta t^4)$ and a current estimate with a systematic error $O(\Delta t^3)$. These systematic errors remain entirely negligible for practical choices of Δt .

More serious are the statistical errors which increase exponentially with time. However by an appropriately large computing effort we were able to control these errors and obtain significant results over time intervals roughly three times those covered in Kraichnan's calculation. This proved to be sufficient to reveal convincingly the asymptotic behaviour of $\alpha(t)$ and $\beta(t)$ even in the most difficult case of frozen turbulence.

In general, using the third-order Runge–Kutta procedure, two updating steps per unit of time was sufficiently accurate, except for $\kappa \geq 0.4$ for which four steps per unit of time were required, to remove systematic errors. The unit of time was chosen to be the lesser of the eddy-circulation time and the velocity-decorrelation time. In fact the results are insensitive to reducing the time step further.

5. Frozen turbulence

Frozen turbulence ($\omega_0 = 0$) is the limiting case most difficult to deal with theoretically. It also represents the most challenging case for simulation since, for vanishing molecular diffusivity κ , important correlations persist over many eddy-circulation periods. In what follows we have set $\omega_0 = 10^{-2}$ for reasons of computational convenience. This represents a timescale considerably longer than any involved in the simulation.

The results for the δ -shell at zero κ are shown in figure 1(a) while figures 1(b) and (c) exhibit the results for a range of values of κ . The corresponding results for the Gaussian model appear in figure 2(a)–(c). Allowing for the difference in scale discussed in §2, the two models clearly show similar behaviour. It should be noted that the results in figure 1(a) confirm those of Kraichnan (1976) up to the end of his time range, which is indicated by the arrow at $\bar{t} = 4$.

The most striking feature of the results is the manner in which $\alpha(t)$ approaches zero for large times when molecular diffusivity is absent. A second important feature is the sensitivity of the asymptotic value of α to the presence of molecular diffusivity. This is exhibited in figures 3(a) and (b). The turbulent diffusivities of the two models (for $\kappa = 0$) are respectively 0.4 and 0.2. We see then that the α -parameter has reached half its maximum at values of κ only 5% of the corresponding turbulent diffusivities. Indeed the maximum value is reached when κ is still at the 25% level.

When κ is comparable to the turbulent diffusivity α begins to conform to the $1/\kappa$ -behaviour predicted by the first-order smoothing approximation (Moffatt 1978, equations 7.41, 7.56 and 7.78). For both models this gives

$$\alpha = -\frac{C}{\kappa} (1 + O(\kappa^{-2})), \quad (5.1)$$

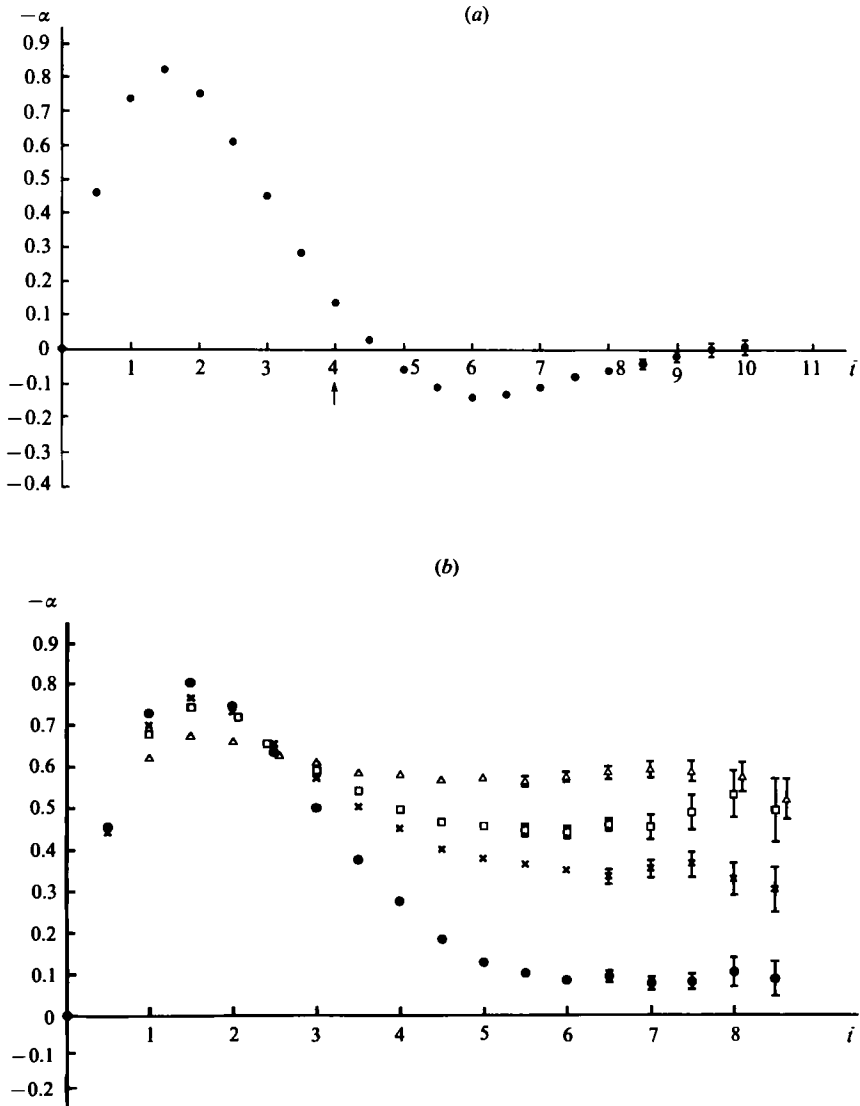


FIGURE 1(a,b). For caption see p. 430.

where, for the δ -shell and the Gaussian respectively, C takes the values 0.167 and 0.088. Figures 4(a) and (b) illustrate the approach of α to its predicted asymptotic form and confirm the $O(\kappa^{-2})$ fractional correction.

In dealing with values of $\kappa \approx 1$ we run into the small systematic discrepancies between values of α derived directly and those from the slope of $\langle \gamma(t) \rangle$. The discrepancy, which appears to behave as $O(\kappa^2 \Delta t^3)$, is not large and is easily controlled by reducing Δt by a factor of 2 in the numerical integration procedure. In fact the indirect method is the less sensitive to Δt .

In figures 5(a) and (b) we exhibit the behaviour of $\beta(t)$ for zero κ . Over the initial time, $t < 4$, it has the same behaviour as found by Kraichnan (1976). (Our values, however, are lower by a factor of two.) On extending the time interval we see that

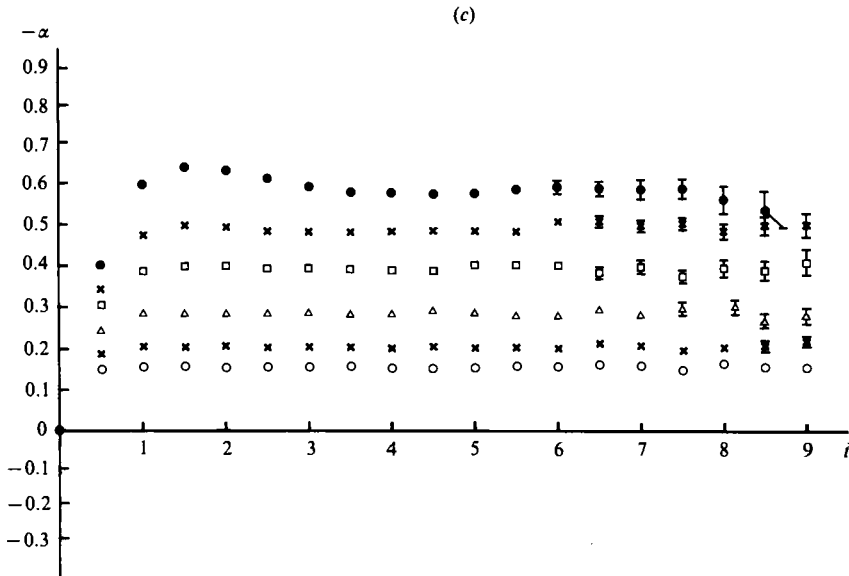


FIGURE 1. $\alpha(t)$ for δ -shell spectrum plotted against $\bar{t} = k_0 t$ for $k_0 = 6$, $\omega_0 = 10^{-2}$, $u_0^2 = 3$, $\psi = \frac{1}{4}\pi$ and for various values of diffusivity. κ values are (a) 0; (b) 0.01 (●), 0.03 (×), 0.04 (□), 0.08 (△); (c) 0.1 (●), 0.2 (×), 0.3 (□), 0.5 (△), 0.75 (×), 1.0 (○). In (a) the arrow indicates the limit of the simulation by Kraichnan (1976). Our results coincide with his up to this point.

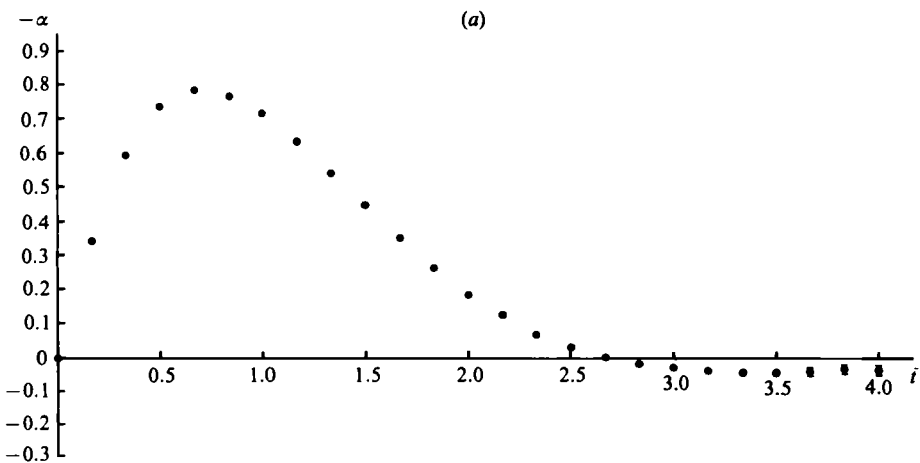


FIGURE 2(a). For caption see facing page.

β continues to oscillate with slowly diminishing amplitude in the δ -shell and rather more rapidly diminishing amplitude in the Gaussian model. We feel that it is plausible to conclude that β approaches zero at large times.

The effect of giving κ a non-zero value is illustrated in figures 5(c) and (d), and in figures 6(a) and (b) we plot the asymptotic values of β against κ omitting some points corresponding to low- κ where it was difficult to pick out an asymptotic value. For $\kappa \geq 1$ the values of β are entirely consistent with the predictions of first-order smoothing for both models (Moffatt 1978, equations 7.41, 7.56 and 7.98).

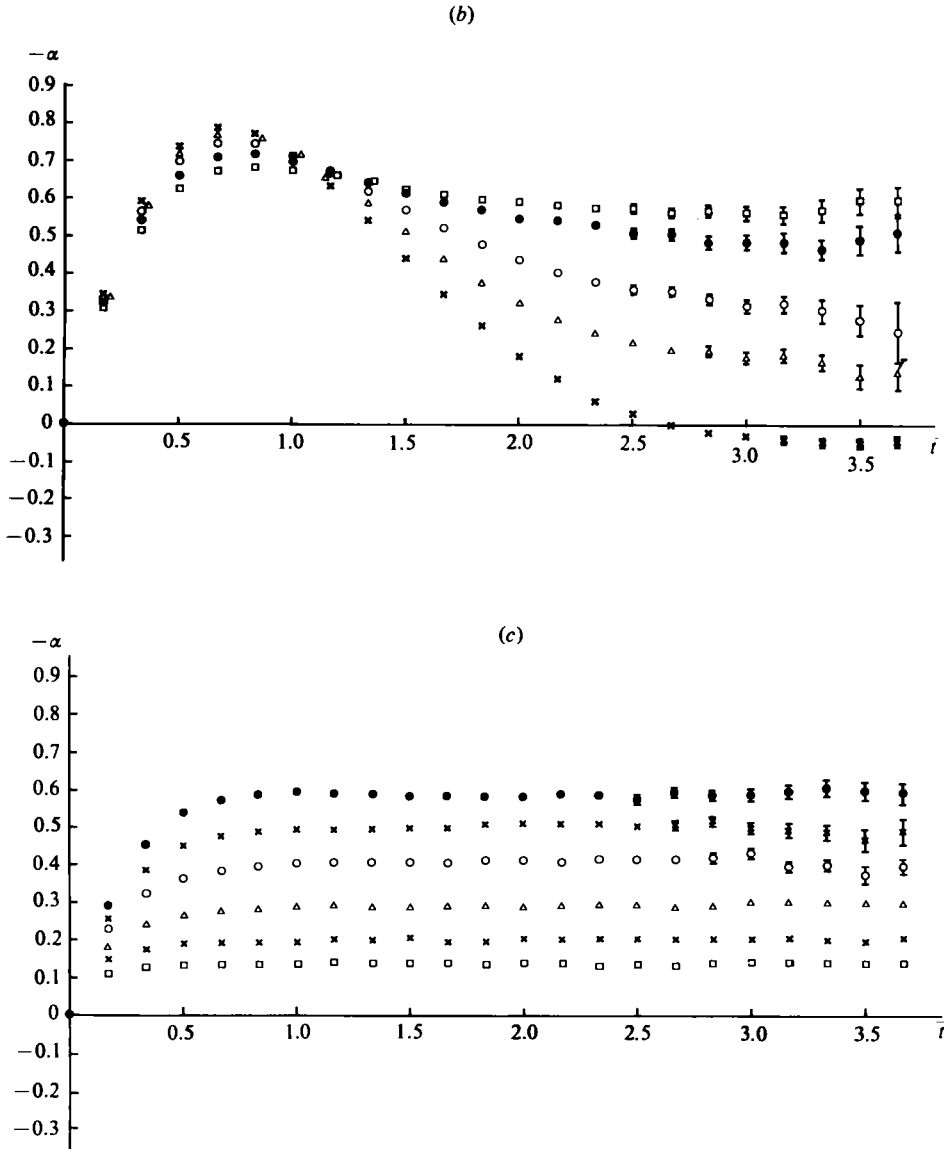


FIGURE 2. $\alpha(t)$ for Gaussian spectrum plotted against $\bar{t} = k_0 t$ for $k_0 = 6$, $\omega_0 = 10^{-2}$, $u_0^2 = 3$, $\psi = \frac{1}{4}\pi$ and for various values of diffusivity. κ values are (a) 0; (b) 0 (\times), 0.005 (Δ), 0.01 (\circ), 0.02 (\bullet), 0.03 (\square); (c) 0.06 (\bullet), 0.1 (\times), 0.15 (\circ), 0.25 (Δ), 0.4 (\times), 0.6 (\square).

6. Non-frozen turbulence

In real turbulence we expect the decorrelation time to be comparable to the eddy-circulation time ($\omega_0 \approx u_0 k_0$). We examined, therefore, the behaviour of $\alpha(t)$ for $\omega_0 = 10$ and various values of κ . Even for $\kappa = 0$, α settled down to an asymptotic value within two eddy-circulation periods. This is consistent with Kraichnan (1976). In figures 7(a) and (b) we show the asymptotic value of α as a function of κ . Note that for large κ the results again approach the predicted curve of the first-order

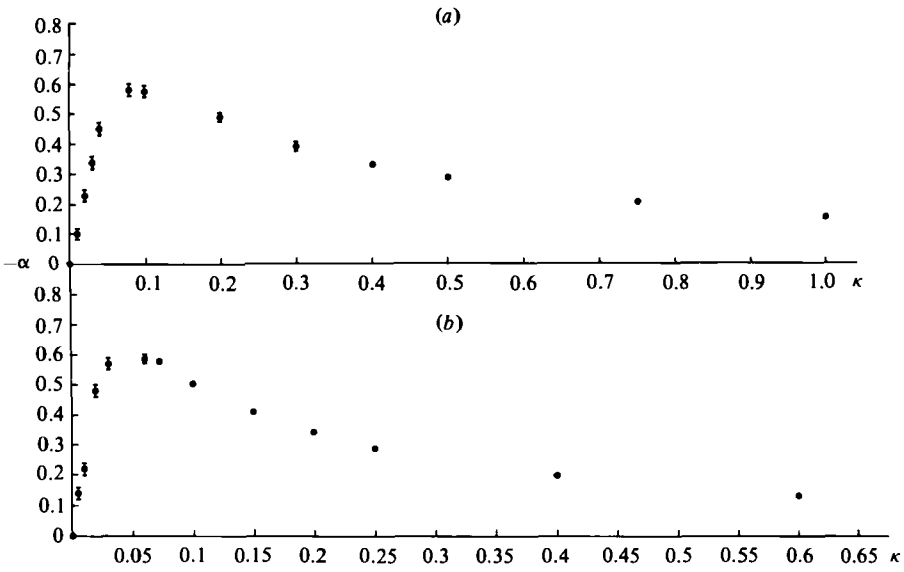


FIGURE 3. $\alpha(\infty)$ plotted against diffusivity κ . (a) δ -shell; (b) Gaussian spectrum.

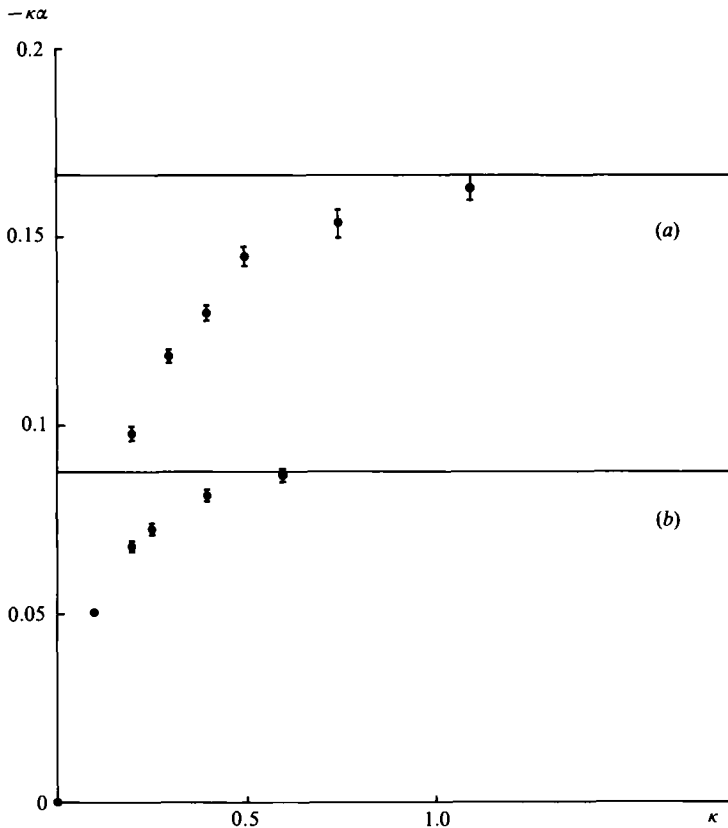


FIGURE 4. $\kappa\alpha(\infty)$ plotted against diffusivity κ for $k_0 = 6$, $\omega_0 = 10^{-2}$, $u_0^2 = 3$, $\psi = \frac{1}{4}\pi$. (a) δ -shell; (b) Gaussian spectrum. The lines show the first-order smoothing result.

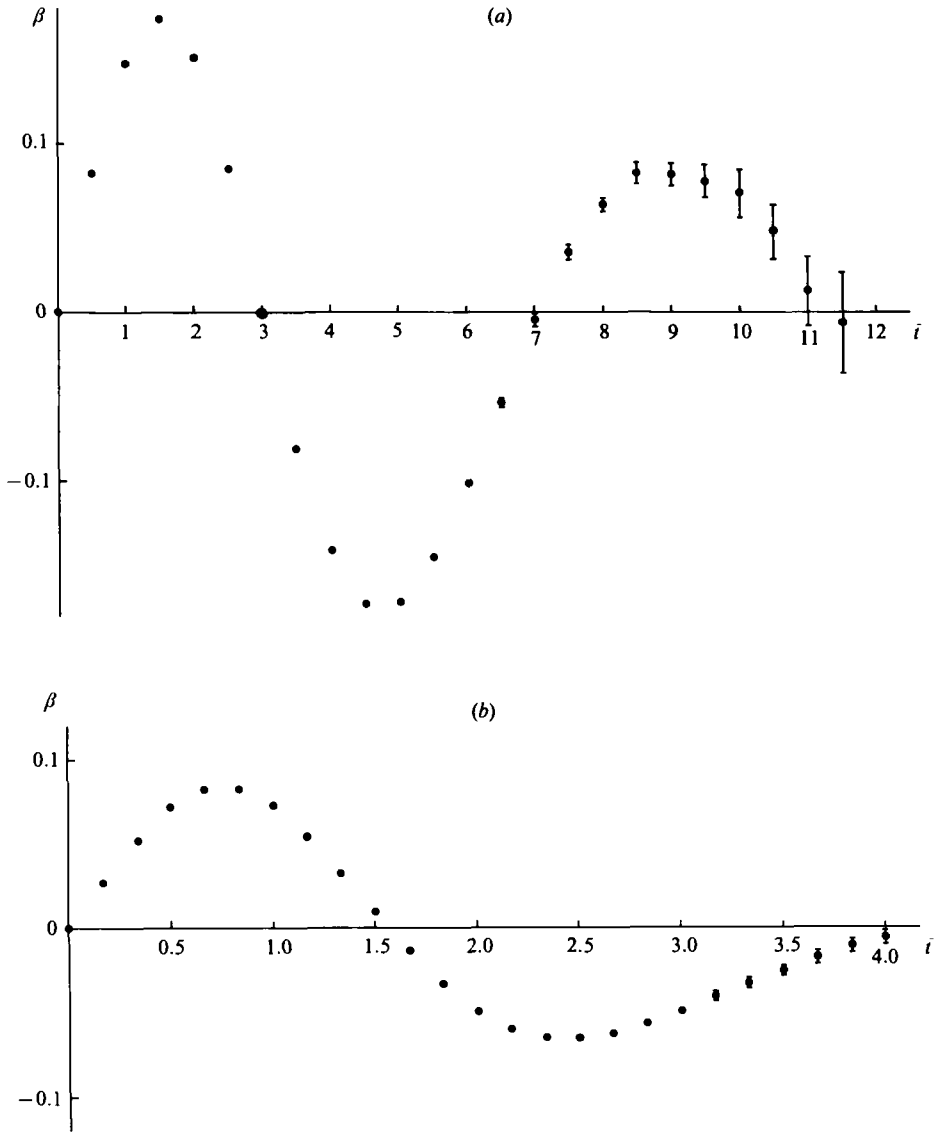


FIGURE 5(a, b). For caption see next page.

smoothing approximation. The same holds for the asymptotic values of β illustrated in figures 8(a) and (b) (Moffatt 1978, equations 7.41, 7.56, 7.78 and 7.98).

We also investigated the dependence of α and β on ω_0 for $\kappa = 0$. The results for α appear in figures 9(a) and (b). The upper end of the range corresponds to the Markovian limit. Here theory suggests (Vainshtein 1970) that

$$\alpha \approx -\frac{1}{6} \int_{-\infty}^{\infty} d\tau \langle \mathbf{u}(\mathbf{x}, \tau) \cdot \nabla \wedge \mathbf{u}(\mathbf{x}, 0) \rangle. \tag{6.1}$$

For the δ -shell this gives

$$\alpha = -\frac{\sqrt{2}}{6} \left(\frac{u_0^2 k_0}{\omega_0} \right), \tag{6.2}$$

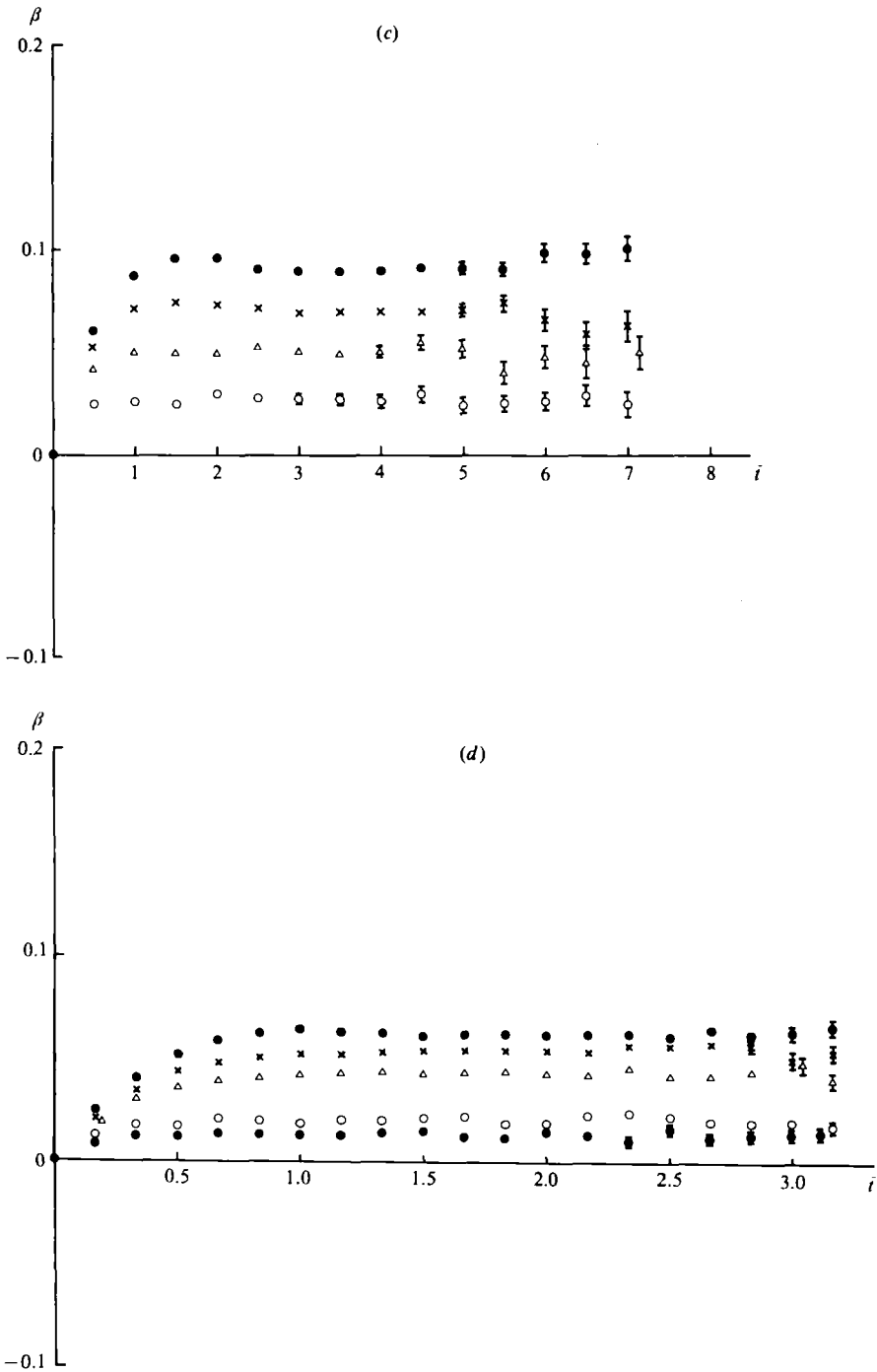


FIGURE 5. $\beta(t)$ plotted against $\bar{t} = k_0 t$ for $k_0 = 6$, $\omega_0 = 10^{-2}$, $u_0^2 = 3$, $\psi = \frac{1}{4}\pi$ and for various values of diffusivity κ . (a) $\kappa = 0$, δ -shell; (b) $\kappa = 0$, Gaussian spectrum; (c) δ -shell, $\kappa = 0.2$ (\bullet), 0.3 (\times), 0.5 (\triangle), 1.0 (\circ); (d) Gaussian spectrum $\kappa = 0.06$ (\bullet), 0.1 (\times), 0.15 (\triangle), 0.4 (\circ), 0.6 (\bullet).

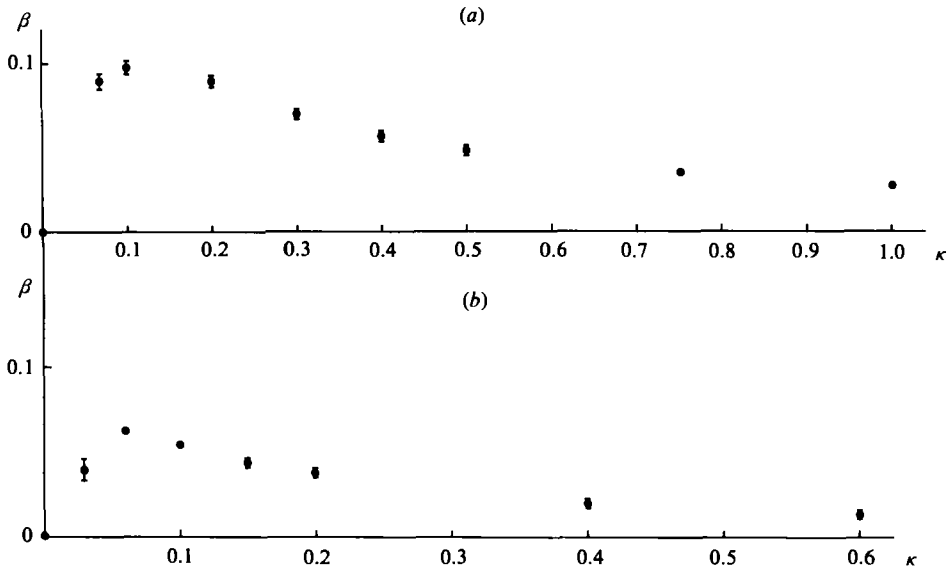


FIGURE 6. $\beta(\infty)$ plotted against diffusivity κ for $k_0 = 6$, $\omega_0 = 10^{-2}$, $u_0^2 = 3$, $\psi = \frac{1}{4}\pi$. (a) δ -shell; (b) Gaussian spectrum.

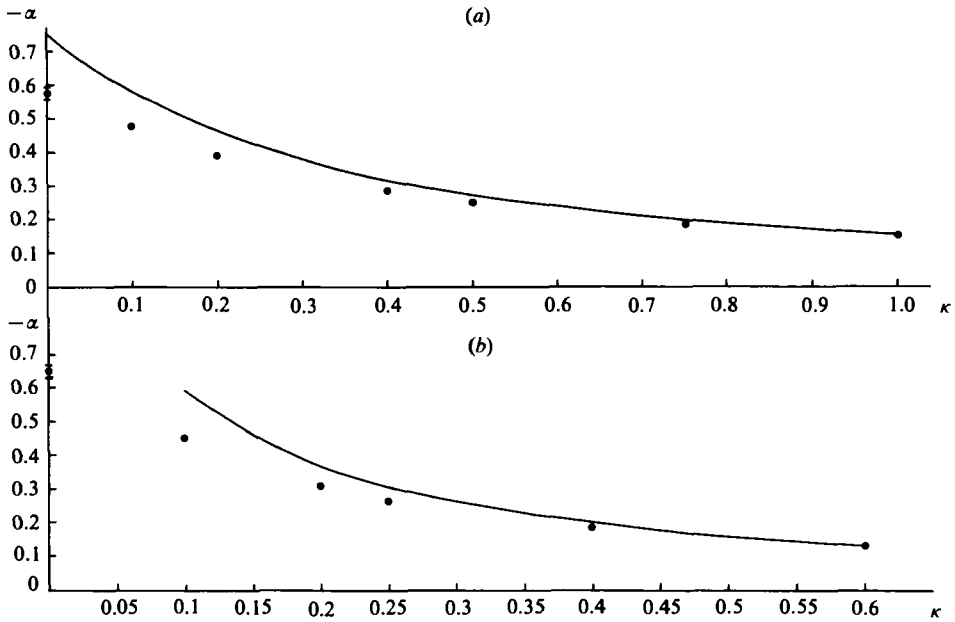


FIGURE 7. $\alpha(\infty)$ plotted against diffusivity κ for $k_0 = 6$, $\omega_0 = 10$, $u_0^2 = 3$, $\psi = \frac{1}{4}\pi$. (a) δ -shell; (b) Gaussian spectrum. The curves show the predictions of the first-order smoothing approximation.

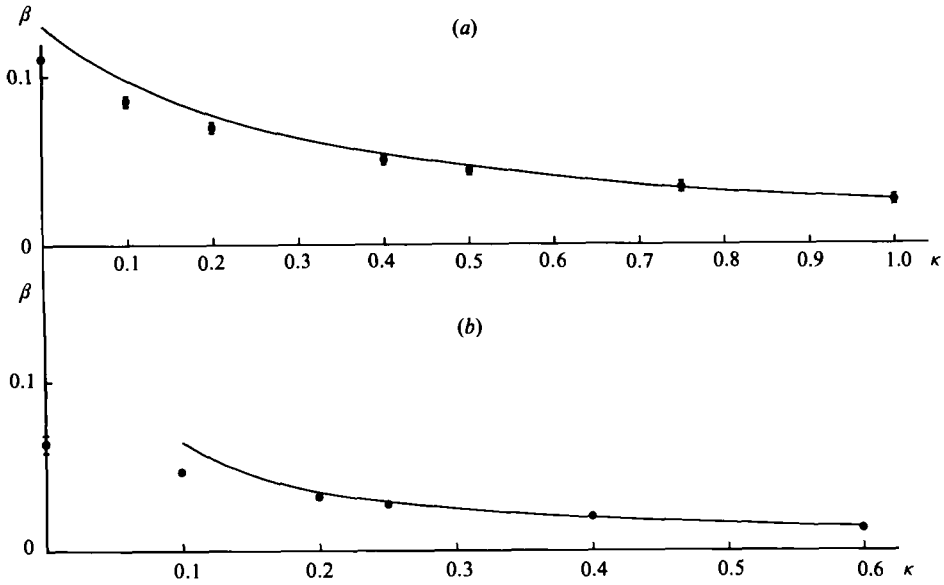


FIGURE 8. $\beta(\infty)$ plotted against diffusivity κ for $k_0 = 6$, $\omega_0 = 10$, $u_0^2 = 3$, $\psi = \frac{1}{4}\pi$. (a) δ -shell; (b) Gaussian spectrum. The curves show the predictions of the first-order smoothing approximation.

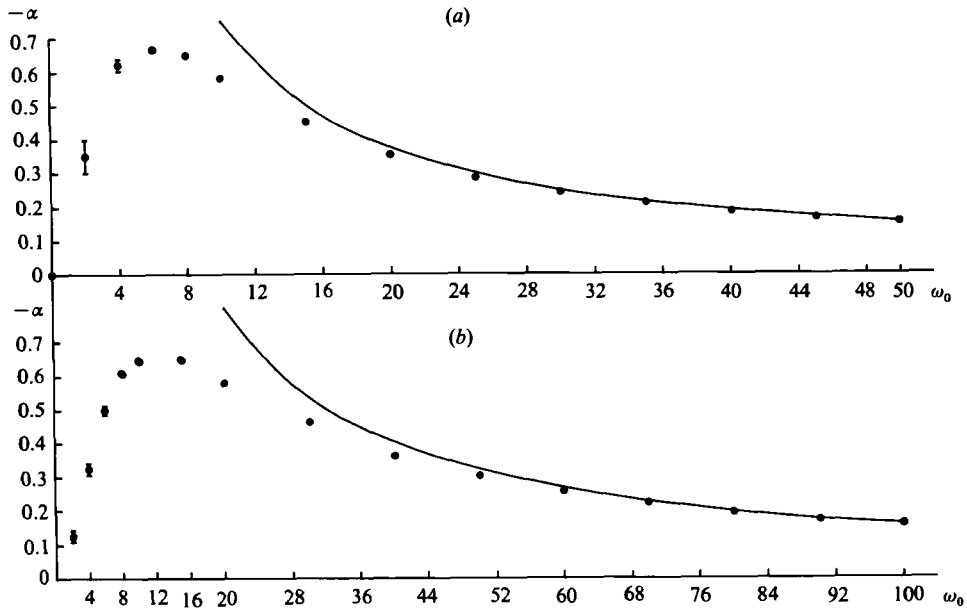


FIGURE 9. $\alpha(\infty)$ plotted against ω_0 for $k_0 = 6$, $\kappa = 0$, $u_0^2 = 3$, $\psi = \frac{1}{4}\pi$. (a) δ -shell; (b) Gaussian spectrum. The curves show the prediction in the Markovian approximation.

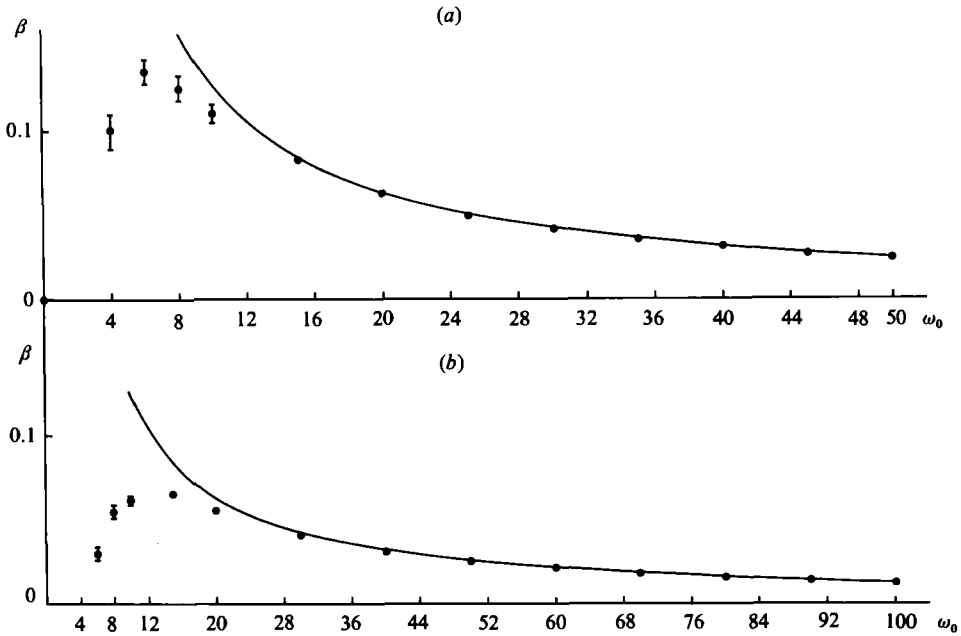


FIGURE 10. $\beta(\infty)$ plotted against ω_0 for $k_0 = 6$, $\kappa = 0$, $u_0^2 = 3$, $\psi = \frac{1}{4}\pi$. (a) δ -shell; (b) Gaussian spectrum. The curves show the prediction in the Markovian approximation.

and for the Gaussian

$$\alpha = -\frac{8}{9} \left(\frac{u_0^2 k_0}{\omega_0} \right). \tag{6.3}$$

Clearly the graphs confirm these results for both models.

In figures 10(a) and (b) the results for β are exhibited. In this case β is expected to be given by the Markovian estimate of the eddy diffusivity for large ω_0 , namely

$$\beta = \frac{1}{6} \int_{-\infty}^{\infty} d\tau \langle \mathbf{u}(\mathbf{x}, \tau) \cdot \mathbf{u}(\mathbf{x}, 0) \rangle. \tag{6.4}$$

That is

$$\beta = \frac{\sqrt{(2\pi)} u_0^2}{6 \omega_0} \tag{6.5}$$

in both cases, a prediction confirmed by our results.

7. Conclusions

The most striking outcome from our simulation is the vanishing, in frozen turbulence, of the α -effect and turbulent magnetic diffusion, in the absence of molecular diffusivity. It is also interesting that both effects appear rapidly when κ is given a non-zero value, rising to 50% of maximum while κ is only 5% of the turbulent diffusivity (Drummond *et al.* 1984), and reaching maximum for κ still at the 25% level. At maximum, κ and the magnetic diffusivity are roughly equal.

For large κ , approximately twice the original turbulent diffusivity, both effects fit well with the predictions of the first-order smoothing approximation (Moffatt 1978).

For non-frozen turbulence we find that both effects remain when κ vanishes, and for short decorrelation times (ω_0 large) the results fit well with the prediction of the Markovian approximation (Vainshtein 1970). When ω_0 is comparable to $u_0 k_0$ both

α and β are smooth monotonic decreasing functions of κ and again approach the first-order smoothing approximation for large κ .

The statistics necessary to achieve our results were, in general, the consequence of following roughly 1.5×10^5 diffusing particle paths. For some points, such as $\alpha(t)$ and $\beta(t)$ at low κ and large times, it was necessary to increase the sample to 4.5×10^6 paths.

It is interesting to speculate on the relationship between our results for frozen turbulence and the discussion by Moffatt (1979) of the Bullard dynamo. He emphasizes the fact that the dynamo effect only occurs when the appropriate parts of the circuit have finite conductivity, thus permitting the magnetic-field transfer across the boundary necessary for flux build-up. This is paralleled by our result that molecular diffusion is necessary in frozen turbulence in order that $\alpha(t)$ may acquire a non-zero asymptotic value, that is, that finite conductivity is necessary for the occurrence of the flux slippage essential for the dynamo effect.

However, as discovered by Kraichnan (1976) and amply confirmed in our simulation, when the turbulence has a finite correlation time a non-vanishing α -effect occurs even in the absence of molecular diffusivity. This is consistent with the results of the Markovian approximation (Vainshtein 1970). Clearly the absence of flux slippage in an actual flow is no barrier to the operation of the dynamo mechanism for the mean field. In fact, as is clear from an analysis of our stochastic equations and as is evident in the work of Molchanov *et al.* (1984), there is no flux slippage at a microscopic level even when molecular diffusivity is present. The randomly jumping particles still carry the field with them. These authors, in effect, use this fact to show that when the decorrelation time is finite we should expect a continuously varying and non-vanishing α -effect even in the infinite-conductivity limit. Clearly what is needed is a convincing analysis of the *frozen* turbulence limit and how it is affected by either molecular diffusivity or finite decorrelation time. We hope our results will provide a good test of any theoretical model in this area.

REFERENCES

- DRUMMOND, I. T., DUANE, S. & HORGAN, R. R. 1984 *J. Fluid Mech.* **138**, 75.
 GREENSIDE, H. S. & HELFAND, E. 1981 *Bell Syst. Tech. J.* **60**, 1927.
 HELFAND, E. 1979 *Bell. Syst. Tech. J.* **58**, 2289.
 KRAICHNAN, R. H. 1976 *J. Fluid Mech.* **77**, 753.
 KRAUSE, F. & RÄDLER, K.-H. 1980 *Mean-Field Magnetohydrodynamics and Dynamo Theory*. Academic and Pergamon.
 MOFFATT, H. K. 1978 *Magnetic Field Generation in Electrically Conducting Fluids*. Cambridge University Press.
 MOFFATT, H. K. 1979 *Geophys. Astrophys. Fluid Dyn.* **14**, 147.
 MOLCHANOV, S. A., RUZMAIKIN, A. A. & SOKOLOFF, D. D. 1984 *Geophys. Astrophys. Fluid Dyn.* **30**, 242.
 VAINSHTEIN, S. I. 1970 *Sov. Phys. J. Exp. Theor. Phys.* **31**, 87.